Sakarya University Journal of Science

ISSN : 2147-835X
Publisher : Sakarya University

Vol. 28, No. 6, 1194-1201, 2024
DOI: https://doi.org/10.16984/saufenbilder.1315557

Research Article

Effect of Cooling Rate on Material Properties in Homogenization Heat Treatment of 6060 Aluminum Alloy

Büşra Gedik, Miraç Alaf*

Bilecik Seyh Edebali University, Faculty of Engineering, Department of Metaluurgical and Materials Engineering, Bilecik, Türkiye, busragdikk@gmail.com, mirac.alaf@bilecik.edu.tr
*Corresponding Author

ARTICLE INFO

Keywords:
Aluminium alloys
Homogenisation
Microstructure
Material properties

Article History:
Received: 20.06.2023
Accepted: 06.11.2024
Online Available: 21.11.2024

ABSTRACT

An important alloy family utilized in the extrusion sector is the 6xxx series of aluminum alloys, which can also be aged through heat treatment. Because of its excellent extrudability, it is easily formable. Before extrusion, formable aluminum alloys are typically heated through homogenization. With the homogenization process applied to the material, it is ensured that the product surface is clean and the microstructure that determines the extrusion speed is obtained with the controlled cooling applied after homogenization. In this study, homogenization heat treatment was carried out in continuous type homogenization furnaces of AA-6060 series Al billet produced with direct chill (DC) casting. In the cooling section, different cooling rates were obtained by changing the speeds of the fans and the effect of the cooling rate on the material properties were examined. According to X-ray diffraction (XRD) results, β-AlFeSi, α-AlFeSi and Mg2Si phases were observed in the alloys. The needle-shaped β-AlFeSi phase seen at the grain boundaries of the casting sample was observed by scanning electron microscope (SEM) and optic microscope (OM), where homogeneously heat-treated samples transformed into spherical form α-AlFeSi at the grain boundaries. Although the cooling rates did not have a significant and significant effect on the microstructure in homogenization, the saving obtained from the total electricity consumption of the turbo fans was 29.6%

1. Introduction

Since the Al-Mg-Si system offers alloys with appealing features, such as low density, medium strength, good ductility, high weldability, strong corrosion resistance and also a relatively low price, the majority of Al extrudates produced today are of the 6xxx series [1]. The 6060 alloy, which is also the most popular one on the European market, is one of the most popular 6xxx alloys [2]. The common usage of 6xxx (Al-Mg-Si) aluminum alloys is primarily due to their excellent mix of medium strength, for industrial applications, and good workability, resulting in great productivity in forming processes[3]. The most extensively used extruded aluminum alloy is AA 6063, which is primarily employed in the building and transportation sectors [4].

The 6xxx line of extrudable aluminum alloys go through a direct-chill casting, homogenization cycle, and hot extrusion process chain [5]. For following mechanical working procedures, such as rolling, drawing, or extrusion, as cast billets of 6xxx aluminum alloys are often unsatisfactory. The as-cast material has microstructural inhomogeneities that result from the solidification process, including elemental microsegregation at the level of the secondary dendrite arms, grain boundary segregation, and the formation of a number of intermetallic and low-melting eutectics [6]. The presence of intermetallic phases, particularly those with sharp edges, can decrease the deformability of 6xxx extrudable alloys, particularly when they are located in grain boundary areas [7].

Cite as: B. Gedik, M. Alaf (2024). Effect of Cooling Rate on Material Properties in Homogenization Heat Treatment of 6060 Aluminum Alloy, *Sakarya University Journal of Science*, 28(6), 1194-1201. https://doi.org/10.16984/saufenbilder.1315557

Consequently, these imperfections reduce the as-cast billet's extrudability [8].

During solidification, particles of β-Al5FeSi, α-Al12(FexMn(1-x))3Si, and Mg2Si are formed in 6xxx Al alloys with Fe, Si, Mg, and Mn alloying elements [9]. The β-Al5FeSi particles are an undesirable phase for further processes, such as billet extrusion. Due to the melting of the β-Al5FeSi phase during extrusion, hot cracking and surface flaws like pickup are brought on, which results in poor surface quality [10]. Before extrusion, as-cast billets undergo heat treatment to produce extruded billets with excellent surface quality [11] .

The main objective of 6xxx homogenization is dissolving coarse primary Mg_2Si precipitates at the grain boundaries in the as-cast state and lowers microsegregation of alloying elements. Another purpose of homogenization is transformation β–AlFeSi → α–AlFeSi. Spheroidization of α-particles also takes place during cooling [12].

In this paper, the effects of changes in the cooling rate of heat-treated billets were examined following the fabrication of AA6060 alloy by the DC casting method. The operation of the fans in the cooling furnace at different speeds during cooling significantly affects the electricity consumption. The aim of the present investigation is to examine whether there is a significant change in the microstructure by saving electricity in the operation of these fans

2. Experimental Details

Billets with a diameter of 152 mm from AA6060 aluminum alloy were produced by DC vertical continuous casting method in industrial conditions. Thermo Fisher Scientific's ARL 'Spark 8820 Optical Emission Spectrometer (OES) was used to establish the alloy's chemical composition, which is shown in Table 1.

Table 1. Chemical composition of AA6060 (%weight)

Alaşım	Si	Mg	Fe	Ti	Mn	Cu	Zn	Al
AA6060	0.52	0.54	0.19	0.01	0.04	0.01	0.02	Balance

After casting process, the billets were subjected to homogenization process in a continuous type furnace. The billets, which were taken into the furnace at room temperature, were kept in the heating chamber for 2 hours until the temperature of the furnace increased to 585 °C, and then in the holding room at 585 °C for 2 hours. As the last step, they were taken to the cooling section with four fans and cooling process was carried out. Different cooling rates were obtained for the billets according to the operating rate of these fans. Table 2 gives the cooling rates of AA6060 billets after homogenization, depending on the operating rates of the fans.

Table 2. Cooling rates of AA6060 billets

Operating Rate of Fans and Sample Codes	Temp. (°C)	Time (min)	Cooling Rate (°C/min)
95%	576	0	11.0
	549	1	
	136	22	
	69	46	
75%	576	0	10.8
	549	1	
	158	22	
	78	46	
55%	576	0	10.5
	549	1	
	186	22	
	91	46	
25%	578	0	10.2
	555	1	
	137	22	
	110	46	

The electricity consumption of the furnace depending on the operating rates of the fans is presented in Table 3. When the speed of the fans is reduced, approximately 36 times lower electricity consumption is remarkable.

The microstructures of the samples were studied with optic microscopy (OM, Nikon Eclıpse LV150N), scanning electron microscopy and energy dispersive spectroscopy (SEM-EDS, JEOL 6060). Porosity ratios and grain sizes were quantified using the CLEMEX image analyzing system. OM and SEM samples were prepared by electropolishing with Barker’s reagent (7 ml HBF_4 ve 93 ml H_2O) at 150-200 mA for 70 s. Phase structure of samples were characterized by X-Ray diffraction (XRD) analysis technique with

CuKα radiation using a RIGAKU D/ MAX 2000 X-ray diffractometer

Table 3. Electricity consumption of the furnace

Fan Ratios	Big Fan Instant Consumption (kW)	Small Fan Instant Consumption (kW)	Total Instant Consumption (kW)
%95	38.29	16.62	109.82
%75	17.67	8.31	51.96
%55	7.37	3.46	21.66
%25	0.98	0.53	3.02

3. Results and Discussion

XRD spectrometry was used for the analysis of the phases of the change in the cooling rate after homogenization of the billet produced from AA6060 alloy. The XRD patterns of the samples taken from the billets that were not heat treated after casting and cooled at four different rates are presented in Figure 1. It has been determined that the peaks obtained as a result of this analysis are the peaks of the planes of the β-AlFeSi, α-AlFeSi and Mg_2Si phases. Peaks at 2Θ= 38°, 44°, 64°, 77° and 82° in all samples were determined by JCDPS card numbers 01-089-2769 belong to the Al peak [13].

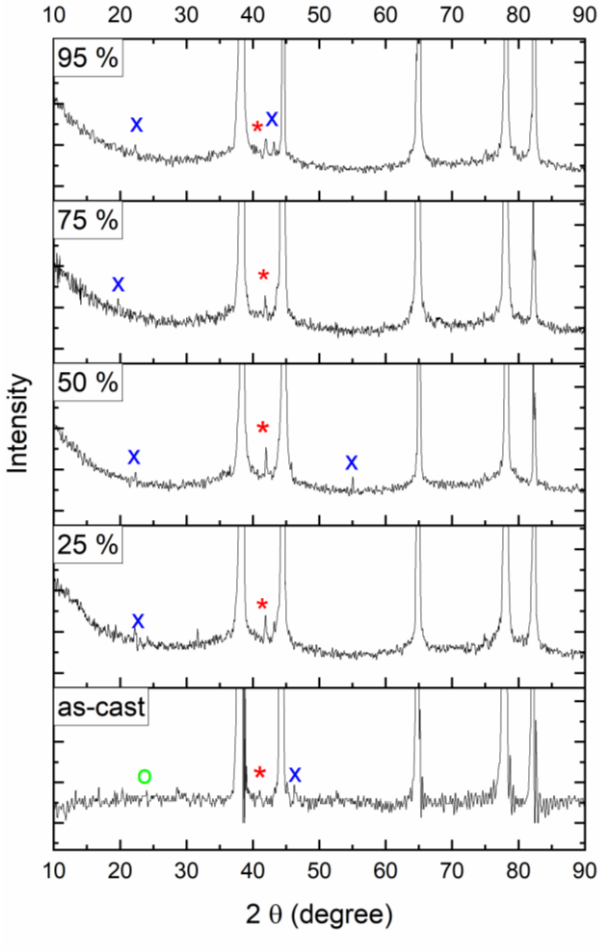

Figure 1. XRD patterns of the samples

Since the amounts of AlFeSi and Mg_2Si phases are very small in the sample, no clear peak outputs were observed in the XRD peaks [8]. According to the XRD pattern, the β-AlFeSi phase (PDF#41-089 denoted "o") was observed at 2Θ= 22° in the untreated specimen after casting. In other samples, α-AlFeSi (PDF#01-071-4015 denoted "x") phase at 2Θ= 22°, 43° and 46° and Mg_2Si (PDF#35-0773 denoted by " * ") at 2Θ= 41° phase is clearly seen [11]. The β-AlFeSi phase present in the sample that was not heat treated after casting transformed into α-AlFeSi phase after heat treatment.

In the homogenization heat treatment after casting, the processes of dissolution of the Mg_2Si phase, conversion of β–AlFeSi→α–AlFeSi and re-precipitation of the Mg_2Si phase occur during cooling [14]. Due to the small amount of these phases in the total mass, the XRD results do not allow a very clear and clear comparison. The presence of existing phases can be clearly demonstrated using an optical microscope and SEM. The α-AlFeSi intermetallic has a cubic crystal structure and a spherical morphology, while the β-AlFeSi intermetallic exhibits a monoclinic structure and a plate (neutral) morphology. This morphology limits the extrudability of the casting billet by causing local cracking and surface defects in the extruded material [15].

The spherical and acicular morphologies of these phases are clearly evident in their microstructure. In the post casting structure, Mg_2Si phase also precipitated at the grain boundaries. This affects the extrusion ability by having a similar effect of the β-AlFeSi phase. During homogenization, the grain boundary Mg_2Si phase dissolves and re-precipitates with a more homogeneous intragranular distribution during homogenization cooling. This is evident in the microstructure

[16]. The Figure 2 shows 500x optical microscope images of the samples.

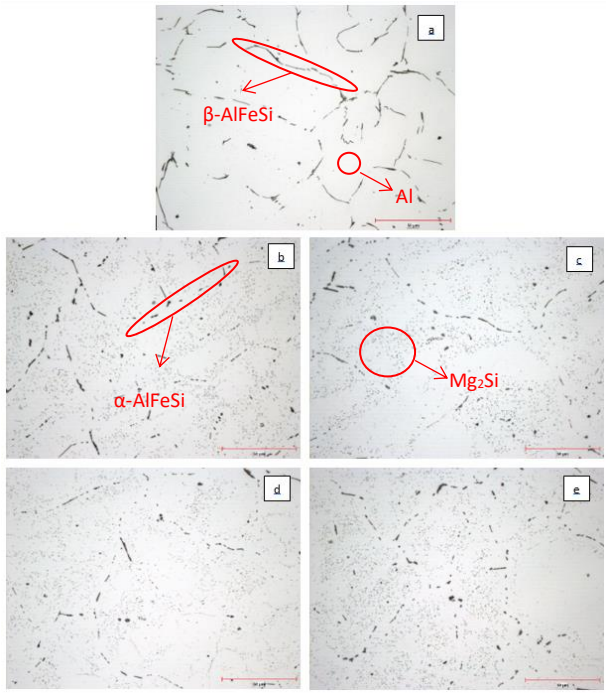

Figure 2. Central Region Microstructure Images at 500x Magnification. (a) as-cast, (b) 95%, (c) 75%, (d) 55, (e) 25%

Looking at the microstructure images in Figure 2, the matrix α-Al phase in the post-cast structure, coarse Mg_2Si particles scattered along grain boundaries and interdendritic spaces, β-AlFeSi phase in plate/needle form at grain boundaries are seen. The light gray areas at the grain boundaries represent the β-AlFeSi phase [17]. It is possible to observe that it is caused by non-equilibrium solidification in the structure in both phases. In the microstructure of the samples that underwent homogenization heat treatment, the β-AlFeSi phase in the form of casting and located at the grain boundaries was replaced by the α-AlFeSi phase in the discrete spherical form. Again, the coarse Mg_2Si phase at the grain boundaries after casting precipitated as small spheres from the grain boundaries into the grain after homogenization heat treatment. The small black dots in the grain represent the Mg_2Si phase [18].

When the microstructures of the cast sample and the homogenized sample are compared, it is observed that the coarse and continuous phases at the grain boundaries of the cast sample precipitate at the grain boundaries in a very fine and fragmented form in the homogenized samples. Mg_2Si phase in the grain boundaries of the casting sample is seen in the microstructures in which the grains precipitate after homogenization. Dark areas indicate AlFeSi phase and light gray areas indicate Mg_2Si phase [8].

Homogenizations a ratio, porosity ratios and grain size analyzes of the produced billets were made with the Clemex software used in conjunction with the optical microscope. The results of the analyzes are shown in Table 4. Accordingly, the change in the homogenization cooling rate did not cause a change in the amount of porosity, homogenization rate and grain size [19] .

Table 4. Homogenization ratios, porosity ratios and particle size analyzes results

Samples	Porosity (%)	Homogenization rate (%)	Grain Size (µm)
95%	0.07	85.64	106
75%	0.06	83.33	105
55%	0.07	84.46	109
25%	0.06	84.17	105
As-cast	0.06	---	107

The Figure 3 shows the SEM photographs of the samples. As seen from the SEM images, the phases in the casting sample (Figure 3.a) are densely located at the grain boundaries. After the homogenization heat treatment (Figure 3.b-e), it is seen that these phases are dispersed into the grain. While the morphology of the phases at the grain boundaries reached a fragmented and spherical structure, the Mg_2Si phase precipitated into the grains as small dots[20].

The EDS results from four different regions of the casting sample of the AA6060 alloy are given in Figure 4. Mg, Al, Si elements were found in line with the qualitative elemental result obtained from the 1st region. The possible phase is Mg_2Si. Mg, Al, Si, Fe elements were found in line with the qualitative elemental results obtained from the 2nd region. The possible phase is AlFeSi. In line with the qualitative elemental results obtained from the 3rd region, Al, Si, Fe elements were found. The possible phase is AlFeSi. In line with the qualitative elemental result obtained from the 4th region, Al element was found. The possible phase is α-Al [21].

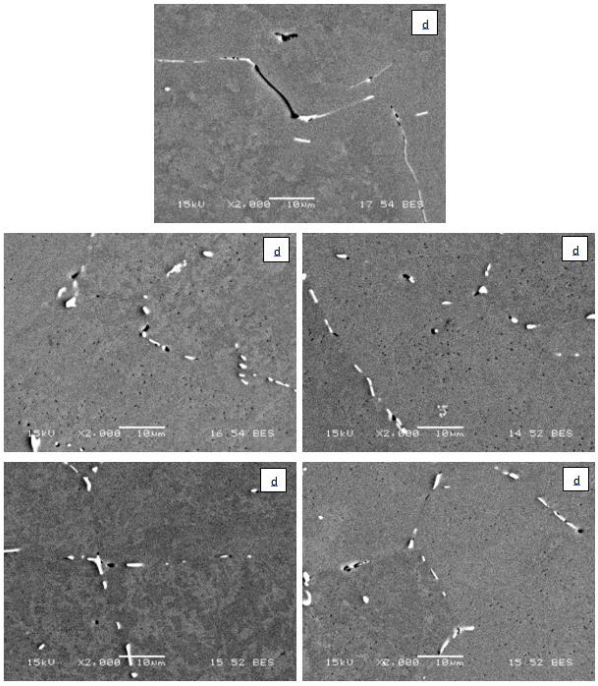

Figure 3. SEM photographs of the samples (a) as-cast, (b) 95%, (c) 75%, (d) 55, (e) 25%

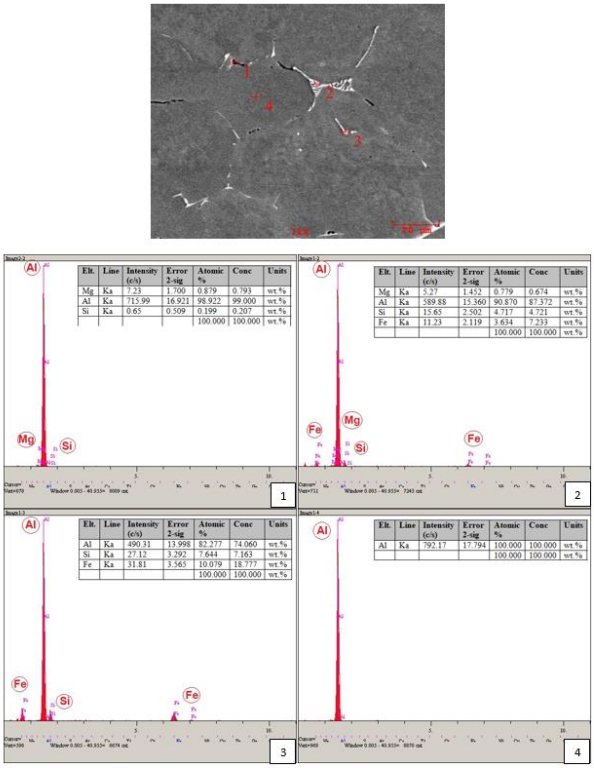

Figure 4. SEM image and EDS spectrums of as-cast sample

The EDS results from two different regions of the 95% sample of the AA6060 alloy are given in Figure 5. Mg, Al, Si elements were found in line with the qualitative elemental result obtained from the 1st region. The possible phase is Mg_2Si. In line with the qualitative elemental result from the 2nd region, Al, Si, Fe elements were found and this possible phase is AlFeSi [12].

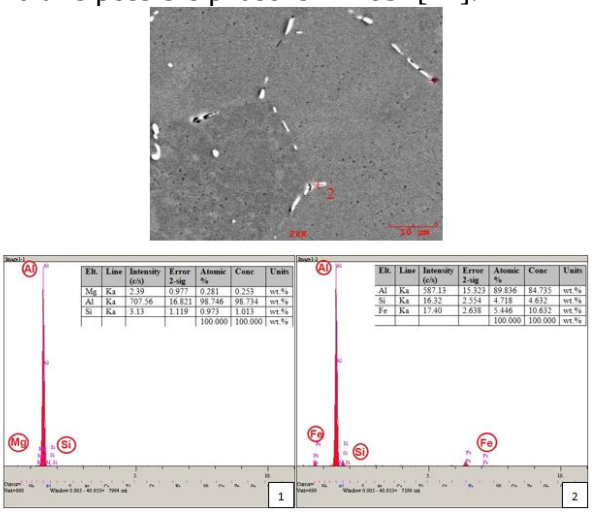

Figure 5. SEM image and EDS spectrums of 95% sample

The elemental analysis results taken from two different regions of the 75% sample of the AA6060 alloy are given in Figure 6 in wt%. Mg, Al, Si elements were found in accordance with the EDS results from the 1st region. The possible phase is Mg_2Si. Mg, Al, Si, Fe elements were found in line with the qualitative elemental result from the 2nd region and this possible phase is AlFeSi.

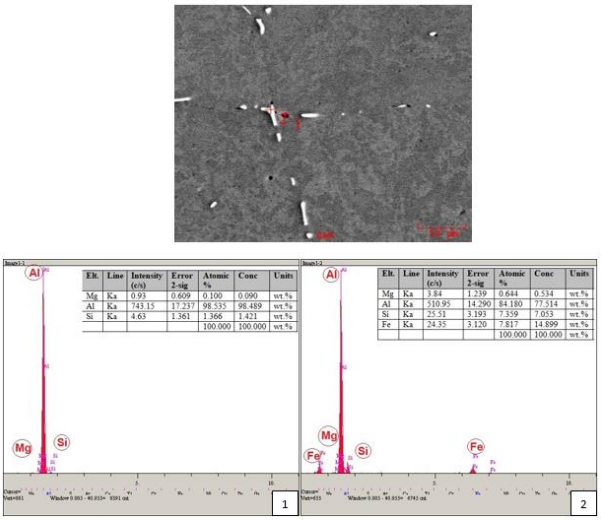

Figure 6. SEM image and EDS spectrums of 75% sample

EDS results from two different regions of 55% sample of AA6060 alloy are given in Figure 7. In line with the qualitative elemental result from the 1st region, Mg, Al, Si elements were found and the possible phase is Mg_2Si. In line with the qualitative elemental result from the 2nd region,

Al, Si, Fe elements were found and the possible phase is AlFeSi [22].

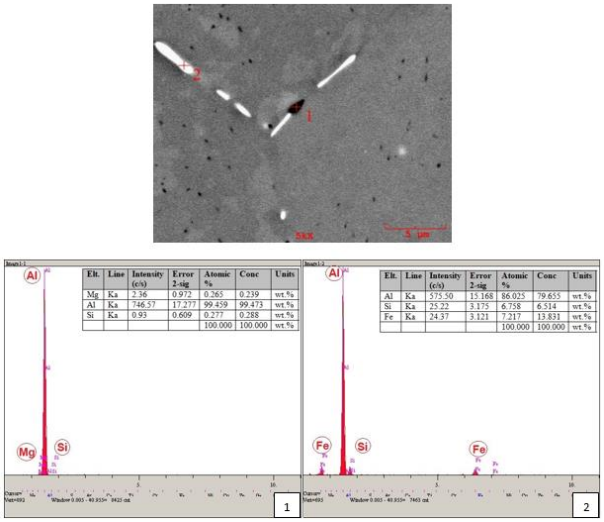

Figure 7. SEM image and EDS spectrums of 55% sample

EDS results taken from two different regions of 25% sample of AA6060 alloy are given in Figure 8. Mg, Al, Si elements were found in line with the qualitative elemental result obtained from the 1st region. In line with the qualitative elemental results obtained from the 2nd region, Al, Si, Fe elements were found. Possible phases are Mg_2Si and AlFeSi, respectively [23].

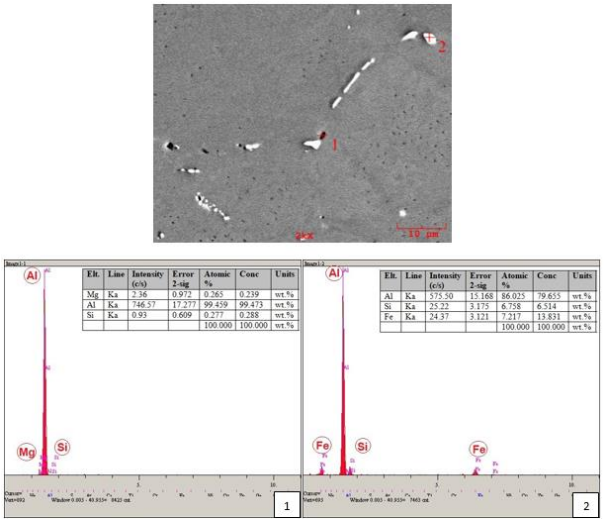

Figure 8. SEM image and EDS spectrums of 25% sample

4. Conclusion

- As the working power of the turbo fans decreases, the cooling rate decreases. By reducing the operating power from 95% to 25%, the cooling rate decreased by 0.08 °C/min.

- Although the cooling rates did not have a significant and significant effect on the microstructure in homogenization, the saving obtained from the total electricity consumption of the turbo fans was 29.6%.

- According to XRD results, β-AlFeSi, α-AlFeSi and Mg_2Si phases were observed in the alloys. The β-AlFeSi phase present in the sample that was not heat treated after casting transformed into α-AlFeSi phase after heat treatment.

- As a result of optical microscope examinations, it has been observed that the needle-shaped β-AlFeSi phase seen at the grain boundaries of the casting sample transforms into spherical form α-AlFeSi at the grain boundaries of the homogeneously heat-treated samples (95%, 75%, 55%, 25%). Likewise, it was determined that the Mg_2Si phase at the grain boundary in the casting sample precipitated into the grains of the homogenization heat-treated structure.

- The average homogenization conversion rate measured with the Clemex software in the optical microscope for the samples cast in AA6060 alloy with a diameter of 152 and a length of 7 m was 84%, the average grain size was 107µm, and the average porosity was 0.06%.

- In the SEM – EDS analysis, matrix α-Al, grain boundaries β-AlFeSi, α-AlFeSi and Mg_2Si phases were determined in the casting sample and the homogenization heat treated samples. It was seen that Mg_2Si phase in dark colors and AlFeSi phase in light colors.

Article Information Form

Acknowledgments
The authors would like to thank Arslan Alüminyum A.Ş. for their support in conducting these experiments.

Funding
The author (s) has no received any financial support for the research, authorship or publication of this study.

Authors' Contribution
BG: Methodology, Conceptualization, Visualization, Writing – Original Draft,

MA: Supervision, Project Administration, Validation, Writing – Review & Editing

The Declaration of Conflict of Interest/ Common Interest

No conflict of interest or common interest has been declared by the authors.

The Declaration of Ethics Committee Approval

This study does not require ethics committee permission or any special permission.

The Declaration of Research and Publication Ethics

The authors of the paper declare that they comply with the scientific, ethical and quotation rules of SAUJS in all processes of the paper and that they do not make any falsification on the data collected. In addition, they declare that Sakarya University Journal of Science and its editorial board have no responsibility for any ethical violations that may be encountered, and that this study has not been evaluated in any academic publication environment other than Sakarya University Journal of Science.

References

[1] I. N. A. Oguocha, A. A. Tiamiyu, M. Rezaei, A. G. Odeshi, J. A. Szpunar, "Experimental investigation of the dynamic impact responses of as-cast and homogenized A535 aluminum alloy.," Materials Science and Engineering A. vol. 771, no. October 2019, p. 138536, 2020.

[2] C. Menapace, F. Bernard, M. Lusa, G. Ischia, G. Straffelini, "Effect of a dual-rate ageing treatment on the tensile properties of a commercial 6060 Al alloy.," Materials Science and Engineering A. vol. 819, no. May, p. 141468, 2021.

[3] S. Liu, J. You, X. Zhang, Y. Deng, Y. Yuan, "Influence of cooling rate after homogenization on the flow behavior of aluminum alloy 7050 under hot compression.," Materials Science and Engineering A. vol. 527, no. 4–5, pp. 1200–1205, 2010.

[4] K. B. S. Couto, M. Goncalves, W. H. Van Geertruyden, W. Z. Misiolek, "Homogenization and Hot Ductiility of Aluminum Alloy AA 6063.," Proceedings of the 9th International Conference on Aluminium Alloys (2004). pp. 1388–1393, 2004.

[5] P. I. Sarafoglou, J. S. Aristeidakis, M. I. T. Tzini, G. N. Haidemenopoulos, "Metallographic index-based quantification of the homogenization state in Extrudable Aluminum alloys.," Metals. vol. 6, no. 5, pp. 1–11, 2016.

[6] J. Miao, S. Sutton, A. A. Luo, "Deformation microstructure and thermomechanical processing maps of homogenized AA2070 aluminum alloy.," Materials Science and Engineering A. vol. 834, no. January, p. 142619, 2022.

[7] X. Qian, N. Parson, X. G. Chen, "Effect of Homogenization Treatment and Microalloying with Mn on the Microstructure and Hot Workability of AA6060 Aluminum Alloys.," Journal of Materials Engineering and Performance. vol. 28, no. 8, pp. 4531–4542, 2019.

[8] P. I. Sarafoglou, A. Serafeim, I. A. Fanikos, J. S. Aristeidakis, G. N. Haidemenopoulos, "Modeling of microsegregation and homogenization of 6xxx Al-alloys including precipitation and strengthening during homogenization cooling.," Materials. vol. 12, no. 9, p. 2019.

[9] Y. Birol, "Optimization of homogenization for a low alloyed AlMgSi alloy.," Materials Characterization. vol. 80, no. Table 1, pp. 69–75, 2013.

[10] T. Greß, T. Mittler, H. Chen, J. Stahl, S. Schmid, N. B. Khalifa, W. Volk, "Production of aluminum AA7075/6060 compounds by die casting and hot extrusion.," Journal of Materials

Processing Technology. vol. 280, no. September 2019, p. 116594, 2020.

[11] N. Bayat, T. Carlberg, M. Cieslar, "In-situ study of phase transformations during homogenization of 6060 and 6063 Al alloys.," Journal of Physics and Chemistry of Solids. vol. 130, no. July 2018, pp. 165–171, 2019.

[12] A. R. Arnoldt, A. Schiffl, H. W. Höppel, J. A. Österreicher, "Influence of different homogenization heat treatments on the microstructure and hot flow stress of the aluminum alloy AA6082.," Materials Characterization. vol. 191, no. July, p. 2022.

[13] P. Priya, "Microstructural evolution during the homogenization heat treatment of 6XXX and 7XXX aluminum alloys.," p. 222, 2016.

[14] Y. Birol, "The effect of homogenization practice on the microstructure of AA6063 billets.," Journal of Materials Processing Technology. vol. 148, no. 2, pp. 250–258, 2004.

[15] H. Demirpolat, S. Akdi, B. Alkan, "The Effect of Homogenization and Chemical Compositions of 6005 and 6082 Aluminium Alloys on The Cold Forming Process.," European Journal of Science and Technology. no. 28, pp. 16–20, 2021.

[16] A. E. Tekkaya, M. Schikorra, D. Becker, D. Biermann, N. Hammer, K. Pantke, "Hot profile extrusion of AA-6060 aluminum chips.," Journal of Materials Processing Technology. vol. 209, no. 7, pp. 3343–3350, 2009.

[17] S. D. Liu, Y. B. Yuan, C. B. Li, J. H. You, X. M. Zhang, "Influence of cooling rate after homogenization on microstructure and mechanical properties of aluminum alloy 7050.," Metals and Materials International. vol. 18, no. 4, pp. 679–683, 2012.

[18] J. Asensio-Lozano, B. Suárez-Peña, G. F. V. Voort, "Effect of processing steps on the mechanical properties and surface appearance of 6063 aluminium extruded products.," Materials. vol. 7, no. 6, pp. 4224–4242, 2014.

[19] X. Qian, X. Li, Y. Li, G. Xu, Z. Wang, "Microstructure evolution during homogenization and hot workability of 7055 aluminum alloy produced by twin-roll casting.," Journal of Materials Research and Technology. vol. 13, pp. 2536–2550, 2021.

[20] H. Tanihata, T. Sugawara, K. Matsuda, S. Ikeno, "Effect of casting and homogenizing treatment conditions on the formation of Al-Fe-Si intermetallic compounds in 6063 Al-Mg-Si alloys.," Journal of Materials Science. vol. 34, no. 6, pp. 1205–1210, 1999.

[21] B. Adamczyk-Cieślak, J. Mizera, K. J. Kurzydłowski, "Microstructures in the 6060 aluminium alloy after various severe plastic deformation treatments.," Materials Characterization. vol. 62, no. 3, pp. 327–332, 2011.

[22] K. Uttarasak, W. Chongchitnan, K. Matsuda, T. Chairuangsri, J. Kajornchaiyakul, C. Banjongprasert, "Evolution of Fe-containing intermetallic phases and abnormal grain growth in 6063 aluminum alloy during homogenization.," Results in Physics. vol. 15, no. July, p. 102535, 2019.

[23] P. I. Sarafoglou, "Simulation and design of the homogenization process of 6xxx extrudable Aluminum alloys Development of design rules for high extrudability by.," p. 2018.